Four-Dimensional Non-Linear Ray Tracing as a Visualization Tool for Gravitational Physics

Daniel Weiskopf*

Institute for Astronomy and Astrophysics†
University of Tübingen

Abstract

In this paper, general relativistic ray tracing is presented as a tool for gravitational physics. It is shown how standard three-dimensional ray tracing can be extended to allow for general relativistic visualization. This visualization technique provides images as seen by an observer under the influence of a gravitational field and allows to probe spacetime by null geodesics. Moreover, a technique is proposed for visualizing the caustic surfaces generated by a gravitational lens. The suitability of general relativistic ray tracing is demonstrated by means of two examples, namely the visualization of the rigidly rotating disk of dust and the warp drive metric.

CR Categories: I.3.8 [Computer Graphics]: Applications—General relativity J.2 [Physical Sciences and Engineering]: Physics—Theoretical astrophysics

Keywords: differential geometry, four-dimensional spacetimes, general relativity, ray tracing, scientific visualization

1 Introduction

Within Einstein's general theory of relativity, gravitation is described geometrically in the form of a four-dimensional curved spacetime which is formulated by the mathematical theory of differential geometry. Light rays are deflected by gravitational sources because of the curvature of spacetime. The bending of light rays can be taken into account by non-linear ray tracing. In this way, images as seen by an observer—a camera—under the influence of a gravitational field can be generated.

The intent of this paper is to show how general relativistic ray tracing can be the basis for various visualization techniques in gravitational physics. First, ray tracing provides an intuitive approach to numerical or analytical results of gravitational physics, which is especially useful for presentations to colleagues or a wider public. Secondly, it allows a systematic investigation of light rays and the underlying geometry of spacetime. Thirdly, fractal structures for light rays can be identified. Fourthly, the properties of a gravitational lens can be explored, especially its caustic structure. The aptitude of these visualization techniques is demonstrated by means of two examples—the rigidly rotating disk of dust and the warp drive metric.

2 Previous and Related Work

In the physics and computer graphics literature, there are some articles concerned with the appearance of objects under the influence of gravitational light deflection. Usually, only well-known metrics are investigated, which are provided in closed form. The first example is the so-called Schwarzschild solution for a spherically symmetric, static distribution of matter. In [16, 7, 14], for example, the appearance of a neutron star or the flight to a black hole are investigated. Gröller[9] gives a generic approach to non-linear ray tracing as a visualization technique. Bryson[4] presents a virtual environment for the visualization of geodesics in general relativity, where examples of the Schwarzschild and Kerr solutions are shown. (The Kerr solution describes the spacetime of a rotating black hole.)

3 Background

In this section, only a very brief overview of the mathematical background of general relativity can be given. For a detailed presentation we refer, e.g., to [13, 19].

A basic concept of differential geometry is the infinitesimal distance ds,

$$ds^2 = \sum_{\mu,\nu=0}^{3} g_{\mu\nu}(\mathbf{x})\, dx^\mu dx^\nu,$$

where $g_{\mu\nu}(\mathbf{x})$ is an entry in a $4 * 4$ matrix—the metric tensor at the point $\mathbf{x}$ in spacetime—and dx^μ is an infinitesimal distance in the μ direction of the coordinate system.

Paths of objects under the influence of gravitation are identical to so-called geodesics. Geodesics are the "straightest" lines in curved spacetime and have extreme lengths. Geodesics are solutions to a set of ordinary second-order differential equations, the geodesic equations,

$$\frac{d^2 x^\mu(\lambda)}{d\lambda^2} + \sum_{\nu,\rho=0}^{3} \Gamma^\mu_{\nu\rho}(\mathbf{x}) \frac{dx^\nu(\lambda)}{d\lambda} \frac{dx^\rho(\lambda)}{d\lambda} = 0, \qquad (1)$$

where λ is an affine parameter for the geodesic line. The Christoffel symbols $\Gamma^\mu_{\nu\rho}$ are determined by the metric according to

$$\Gamma^\mu_{\nu\rho}(\mathbf{x}) = \frac{1}{2} \sum_{\alpha=0}^{3} g^{\mu\alpha}(\mathbf{x}) \left(\frac{dg_{\alpha\nu}(\mathbf{x})}{dx^\rho} + \frac{dg_{\alpha\rho}(\mathbf{x})}{dx^\nu} - \frac{dg_{\nu\rho}(\mathbf{x})}{dx^\alpha} \right),$$

with $g^{\mu\alpha}(\mathbf{x})$ being the inverse of $g_{\mu\alpha}(\mathbf{x})$.

This paper is focused on a special type of geodesics which are denoted lightlike or null geodesics. The null geodesics are of great importance because they determine the causal structure of spacetime, i.e., they separate regions which cannot have any causal influence on a given point in spacetime. Light rays are identical to these null geodesics. They obey the null condition

$$g_{\mu\nu}(\mathbf{x}) \frac{dx^\mu(\lambda)}{d\lambda} \frac{dx^\nu(\lambda)}{d\lambda} = 0. \qquad (2)$$

In the ray tracing program, the initial position in spacetime and the initial spatial direction of the light ray are determined by the position, orientation, and field of view of the observer's camera and

*weiskopf@tat.physik.uni-tuebingen.de

†Institute for Astronomy and Astrophysics, Section Theoretical Astrophysics, University of Tübingen, Auf der Morgenstelle 10, D-72076 Tübingen, Germany

by the coordinates of the corresponding pixel on the image plane. The time component of the initial direction is fixed by the null condition (2). Therefore, the geodesic equations (1) yield an initial value problem for ordinary differential equations. There exist well-known numerical methods for solving this problem, cf., e.g., [17].

A common problem in general relativity is that many terms depend on the chosen coordinate system and do not have a direct physical or geometric interpretation; for example, this is true for the spatial and temporal coordinates or the metric itself. A major advantage of ray tracing is its independence of the coordinate system. The final images are results of a *gedankenexperiment*: What would an observer see, what would a camera measure? Hence, the images have an immediate physical meaning and are coordinate-free.

This paper is focused on visualizing the geometric structure of light rays in a gravitational field. Therefore, only visual distortions due to gravitational light bending are considered. Changes of color due to the Doppler effect and gravitational redshift, as well as changes of the intensity of the incoming light are neglected.

4 General Relativistic Ray Tracing

The implementation of general relativistic ray tracing is based on *RayViS*[10], which is an object-oriented and easily extensible ray tracing program written in C++. In *RayViS*, all relevant parts of the visualization system are derived from abstract basis classes which allow the extension of the original functionality by subclassing.

Figure 1 shows the basic structure of the program. The image plane is sampled by the `Sample Manager` which uses the `Projector` to generate a `Ray` corresponding to the pixel under consideration. The `Ray` communicates with the `Scene` in order to find intersections with scene objects, calculate secondary rays and shadow rays, and determine illumination. Finally, the resulting color is stored in the image by the `Sample Manager`.

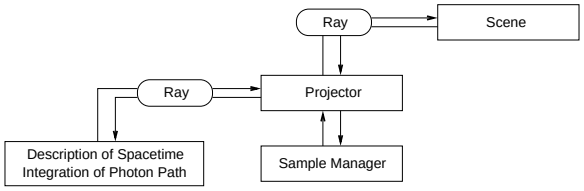

Figure 1: Structure of the ray tracing system.

Relativistic rendering requires two major extensions of the standard three-dimensional Euclidean ray tracing system.

First, the standard ray class which represents a straight light ray in three dimensions is replaced by a class which represents a bent light ray in four dimensions. This bent ray is approximated by a polygonal line whose points possess one temporal and three spatial coordinates.

Secondly, the standard ray projector which generates a light ray corresponding to a pixel on the image plane has to be modified. The new projector provides the interface to the physics of spacetime and communicates with the solver for the geodesic equations (1). This system of ordinary differential equations can be solved by numerical integration. The standard technique in our implementation is the Runge-Kutta method of fourth order[17]. Here, any physical configuration can be examined by replacing the module which supplies the information about the metric and the Christoffel symbols. The advantage of this modular and object-oriented concept is a freedom of choice of the simulated system, combined with a complete, sophisticated rendering environment and only minimal extra implementation costs.

In standard three-dimensional ray tracing, rendering time is significantly determined by the computation of intersections between rays and objects. This is not true for general relativistic ray tracing because here the generation of bent light rays by solving the geodesic equations plays an even more dominant role. Usually, general relativistic ray tracing is a couple of magnitudes slower than non-relativistic ray tracing. Therefore, parallelization is an urgent need for general relativistic ray tracing. Fortunately, the computation of the null geodesics and the ray–object intersections for one pixel is independent of those for the other pixels. Hence, parallelization is performed on a per-pixel basis and utilizes a domain decomposition on the image plane. The granularity can be as fine as a single pixel in order to achieve good load balancing. The implementation makes use of MPI[12] and thus is platform-independent. It scales well, even up to a several hundred nodes on a massive-parallel architecture such as the CRAY T3E.

5 Gravitational Lensing and Caustics

Gravitational fields bend light rays and can thus play the role of a lens—a gravitational lens. Gravitational lensing was early predicted by Einstein himself. In fact, the light deflection measured during the total eclipse of the sun in 1919 was the first experimental evidence for general relativity. Today gravitational lenses are a hot topic in astronomy and are extensively used in observations in various ways. A comprehensive presentation of gravitational lensing can be found in [18].

The main difference between optical lenses and gravitational lenses is that the deflection caused by a typical, spherical convex, optical lens increases with the distance of the ray from the optical axis, whereas the deflection caused by a gravitational lens decreases with the impact parameter. A standard optical lens has a focal point onto which rays parallel to the optical axis are focused. In contrast, a gravitational lens has no focal point. However, the qualitative behavior of a gravitational lens can be described by its caustic surfaces. A gravitational lens might bend light rays in a way that the light emitted by the same source can follow different trajectories to reach the observer, i.e., the light source is projected onto multiple points on the observer's image plane. A caustic surface separates regions where the image multiplicity changes.

Standard gravitational lensing theory uses a couple of approximations which are valid for most astrophysical objects. For example, only small angles of deflection are allowed, the mass distribution is assumed to be nearly stationary, and the mass of the lens and the image source are considered to be projected onto planes—the lens plane and the source plane, respectively. Based on these approximations, the observed data is normally analyzed to reconstruct the properties of the source or the lens, e.g., its mass distribution.

In this paper, a different approach is pursued. First, image synthesis is used instead of analysis. We aim at visualizing a known gravitational field to gain further insight in its characteristics. Secondly, the approximations from above are dropped and the geodesic equations are completely solved. In this way, one can deal with phenomena related to strong gravitational fields, large angles of deflection, and extended and rotating gravitating objects.

We have studied two means of visualizing gravitational lenses. The first technique directly utilizes general relativistic ray tracing. Here, objects are placed around the gravitational lens as image sources. The mapping of these background objects reveals distortions due to gravitational light deflection and a possible multiplicity of points in the image plane. In this way, it provides some information about the structure of the caustics.

We propose a second technique which targets at a more systematic analysis of the caustic surfaces. The deficiency of the first method is that the background objects are only two-dimensional and thus cannot visualize the caustic surfaces embedded in three-dimensional space. This problem can be overcome by a three-dimensional volumetric object which determines the image mul-

tiplicity for points inside and thus samples the volume for caustic structures.

The procedure is as follows. In *RayViS*, both surface and volume objects are supported. A standard volume object is subclassed to additionally store the number and the initial directions of the light rays crossing a voxel of the object. Whenever a voxel is traversed by a ray, a counter is incremented and the position of the pixel on the image plane corresponding to the current ray is attached to this voxel. In a post processing step, each single voxel is evaluated and the number of rays coming from different areas of the image plane are accumulated. In this way, unintentional counting of nearby rays which cross the same voxel is avoided. The minimal required distance on the image plane is specified by the user; usual values are some ten pixels. Currently, only a regular grid is implemented as a caustic finder.

The scalar field containing the image multiplicities is written to a file and visualized by an external program. There exist numerous techniques for volume visualization. We tested isosurface representations based on the marching cube algorithm, and direct volume rendering based on ray casting or, alternatively, shear warp factorization. Isosurfaces directly indicate a change of multiplicity and thus are useful for representing caustic surfaces. Conversely, volume rendering is able to show several caustic structures embedded in one another. Here, shear warp rendering is mainly used for interactive explorations, whereas the ray casting program provides images of higher quality, as for illustrations.

In contrast to general relativistic ray tracing of the previous section, the caustic finder provides coordinate-dependent data. This might give interpretation problems in regions of high curvature. Therefore, this visualization technique is best suited for almost flat parts of spacetime, for example behind the gravitational lens at adequate distance. High computational and memory costs for a fine sampling of the volume grid are another problem, which could be solved by utilizing an adaptive grid.

6 Application: Rigidly Rotating Disk of Dust

The first application presented in this paper is the visualization of the so-called general relativistic rigidly rotating disk of dust, which is a simple model for a galaxy or a galaxy cluster. This project is joint work with the group for gravitational theory at the University of Jena, in particular, with M. Ansorg.

In 1995, Neugebauer and Meinel[15] from Jena succeeded in finding the global, analytical solution of Einstein's equations for the gravitational field of a rigidly rotating (i.e., the angular velocity is independent of the radial position) pressure-free ideal fluid disk—the rigidly rotating disk of dust. The researchers in Jena studied the properties of the corresponding geometry of spacetime, for example, by investigating the trajectories of particles[2].

The cooperation between the theoretical relativists from Jena and our visualization group is motivated by the following reasons. First, there is great interest in "seeing" the results of theoretical work in order to gain some intuitive feeling. Secondly, visualization allows a compact representation of a vast number of null geodesics which are used as another means of probing the gravitational field. Thirdly, the communication of the theoretical research to colleagues and to the public should be facilitated.

Results[20] of the cooperation were presented to the relativity community at the Journées Relativistes '99[11], an international conference on gravitation. The film shown at the Journées Relativistes '99 is also included in the accompanying video. Several visualization techniques which were applied to the rigidly rotating disk of dust are presented in the following.

6.1 Outside View

The first and straightforward approach to visualizing a given gravitational field is to adopt an outside position. Figure 2 illustrates such an outside view. The three images show the disk with varying parameter μ. This parameter describes the relativistic "character" of the disk. For $\mu = 0$ the Newtonian, non-relativistic limit is obtained, for $\mu \approx 4.6$ the ultra-relativistic limit. The parameter μ is defined in [15].

The left image presents an almost Newtonian, classical situation with $\mu = 0.1$. The top side of the disk is colored blue. An artificial "pie slice" texture is applied in order to visualize rotational distortions. The middle image shows a slightly relativistic case with $\mu = 0.7$. Due to gravitational light bending, both the top and the bottom faces are simultaneously visible. The bottom side is colored green and brown. The right image shows a more relativistic situation with $\mu = 3$. Here, multiple images of the top and the bottom emerge. Moreover, rotational distortions which are caused by frame dragging (a general relativistic effect) and by the finite speed of light and the rotation of the disk are prominent.

The outside view gives a first, intuitive approach to the gravitating object. This visualization technique can easily be used for any metric and provides a coordinate-independent result. Furthermore, it is most useful for presenting the theoretical research to the public. For example, pictures of the rigidly rotating disk of dust were published in a scientific calendar[6].

6.2 Parameter Study

After these first visualization steps a systematic investigation of the properties of the light rays in the metric of the rigidly rotating disk of dust is required in order to obtain reliable scientific results. Therefore, a sampling of the parameter space for the null geodesics has to be considered.

The null geodesics are determined by two types of parameters. Parameters of the first kind describe the gravitational source. The properties of the disk of dust are completely determined by the parameter μ. The position of the observer and the direction of the incoming light constitute parameters of the second kind. The sampling of the direction of the light rays is implemented in the form of a 4π sterad camera, i.e., an observer looking in all directions simultaneously. Here, the projection onto a virtual sphere surrounding the observer is used instead of the standard projection onto an image plane. Therefore, the parameter space is completely sampled by generating 4π sterad images for various values of μ and positions of the observer.

The produced panorama images are viewed with a simple, external, OpenGL-based rendering program which maps these images onto a sphere. The viewpoint is located at the center of the sphere.

The parameter study confirms the qualitative results from the previous subsection, i.e., multiple images of the top and the bottom side and rotational distortions. In addition, new interesting results were found for disks with sufficiently large values of μ. These results are described in the following subsection.

6.3 Fractal Structure

The most interesting finding of the parameter study is the existence of fractal structures created by the gravitational field of the rigidly rotating disk of dust. Figure 3 shows a typical example. Here, the position of the observer and the parameter $\mu = 3$ are fixed. The observer is located on the axis of symmetry and looking towards the edge of the disk. The leftmost picture shows a snapshot with a wide angle field of view. Parts of the top side of the disk are visible in the lower part of the picture. An image of the bottom side is found directly above this first image of the top side. Further above, alternating images of the top and the bottom faces follow. The pictures

to the right document increasing zooming in on the original picture, whereas the rightmost image shows a part of the leftmost image which has a size approximately ten orders of magnitude smaller than the original image. This series reveals self-similarity and a fractal structure.

6.4 Caustics

Figure 4 shows the structure of the caustic surfaces for $\mu = 0.3$, based on the volumetric method from Sect. 5. The regular grid of the caustic finder has a size of 256^3 voxels. The red colors represent regions with many image multiplicities, the green colors represent regions with fewer image multiplicities, and the blue colors show regions with an image multiplicity of one.

7 Application: Warp Drive

The second application presented in this paper is the visualization of the warp drive metric. Alcubierre's solution[1] of Einstein's field equations allows to travel faster than the speed of light, as measured in an outside, flat region of spacetime. Ford and Roman[8] give a comprehensible introduction the warp metric and a discussion of some issues related to energy conditions and causality.

Basically, the warp drive constructs a warp bubble which separates two flat parts of spacetime. The warp bubble is able to move faster than the speed of light with respect to an outside, flat region of spacetime. A spaceship which is at rest inside the warp bubble would then travel faster than the speed of light.

The visualization of the warp drive was produced for "Seven Hills"[3]. This exhibition intends to give an inkling of what the future of mankind may look like in the next millennium. A leading-edge topic of physics like the visualization of the warp metric is very well suited for such an exhibition and allows to bring aspects of a complex scientific content to a wide public.

Figure 5 and the accompanying video show examples of the visualization of the warp metric. Here, the warp spaceship travels in front of the earth and moon, and Saturn. The light deflection at its warp bubble causes astonishing visual distortions on the background objects. In addition to this outside view, a position inside the warp bubble can be adopted. Respective images are shown at the exhibition "Seven Hills". The view from inside the warp spaceship was independently investigated by Clark et al.[5] on a more theoretical footing.

8 Conclusion and Future Work

In this paper, non-linear ray tracing has been presented as a tool for gravitational physics. It has been shown how standard three-dimensional ray tracing can be extended to general relativistic ray tracing. Furthermore, a parallel implementation has been described, which is extremely useful for extensive parameter studies or production of movies.

General relativistic ray tracing offers several important features. First, it gives an intuitive approach to the structure of a gravitational field and allows a simple and straightforward use. Secondly, the generated images are coordinate-independent and can be regarded as the result of an experiment. This is of great importance in the context of general relativity because many properties of spacetime can be hidden by the normally used coordinate-dependent representation. Many other visualization techniques are based on specific coordinate systems, e.g., the visualization of geodesics with respect to pseudo-Euclidean coordinates in [4]. Thirdly, the ray-traced images are a compact representation of a vast number of null geodesics. These null geodesics probe the properties of spacetime, especially its causal structure. Moreover, an extension has been proposed to visualize the caustic surfaces of a gravitational lens.

By means of two applications the usability of general relativistic ray tracing has been demonstrated both for obtaining further insight by the researcher and for presenting results to colleagues and the public.

In future work, the change of color due to the Doppler effect and gravitational redshift, as well as the change of intensity of the incoming light will be implemented. Furthermore, adaptive algorithms and data structures for the caustic finder will be investigated.

Acknowledgments

This work was supported by the Deutsche Forschungsgemeinschaft (DFG) and is part of the project D4 within the Sonderforschungsbereich 382. Thanks to M. Ansorg and D. Moran for their cooperation and the friendly reception in Jena. The production of the warp drive visualization was supported by the Berliner Festspiele GmbH; thanks to R. Bülow for the kindly collaboration.

References

[1] M. Alcubierre. The warp drive: hyper-fast travel within general relativity. *Classical and Quantum Gravity*, 11:L73–L77, 1994.

[2] M. Ansorg. Timelike geodesic motions within the general relativistic gravitational field of the rigidly rotating disk of dust. *Jounal of Mathematical Physics*, 39(11):5984–6000, 1998.

[3] Berliner Festspiele GmbH. *Seven Hills. Images and Signs of the 21st Century.* Exhibition, 14 May to 29 October 2000, Berlin. Web Site: http://www.berlinerfestspiele.de/berlinzweitausend/seven.html.

[4] S. Bryson. Virtual spacetime: An environment for the visualization of curved spacetimes via geodesic flows. In *Proceedings of Visualization '92*, pages 291–298, 1992.

[5] C. Clark, W. A. Hiscock, and S. L. Larson. Null geodesics in the Alcubierre warp-drive: the view from the bridge. *Classical and Quantum Gravity*, 16:3965–3972, 1994.

[6] Deutsche Forschungsgemeinschaft (DFG). Kalender 2000 (calendar 2000), Bonn, 2000.

[7] T. Ertl, F. Geyer, H. Herold, U. Kraus, R. Niemeier, H.-P. Noller, A. Rebetzky, H. Ruder, and G. Zeller. Visualization in astrophysics. In *Eurographics '89 Proceedings*, pages 149–158, 1989.

[8] L. H. Ford and T. A. Roman. Negative energy, wormholes and warp drive. *Scientific American*, pages 30–37, Jan. 2000.

[9] E. Gröller. Nonlinear ray tracing: Visualizing strange worlds. *The Visual Computer*, 11(5):263–276, 1995.

[10] A. Gröne. *Entwurf eines objektorientierten Visualisierungssystems auf der Basis von Raytracing*. PhD thesis, University of Tübingen, 1996.

[11] *Journées Relativistes '99*. International European Conference on Gravitation. Web Site: http://www.tpi.uni-jena.de/tpi/journees-relativistes.html.

[12] *Message Passing Interface Forum*. Web Site: http://www.mpi-forum.org.

[13] C. W. Misner, K. S. Thorne, and J. A. Wheeler. *Gravitation*. Freeman, New York, 1973.

[14] R. J. Nemiroff. Visual distortions near a neutron star and black hole. *American Journal of Physics*, 61(7):619–632, july 1993.

[15] G. Neugebauer and R. Meinel. General relativistic gravitational field of a rigidly rotating disk of dust: Solution in terms of ultraelliptic functions. *Physical Review Letters*, 75:3046, 1995.

[16] H.-P. Nollert, H. Ruder, H. Herold, and U. Kraus. The relativistic "looks" of a neutron star. *Astronomy and Astrophysics*, 208:153, 1989.

[17] W. H. Press, S. A. Teukolsky, W. T. Vetterling, and B. P. Flannery. *Numerical Recipes in C*. Cambridge University Press, second edition, 1994.

[18] P. Schneider, J. Ehlers, and E. E. Falco. *Gravitational Lenses*. Springer, Berlin, 1992.

[19] S. Weinberg. *Gravitation and Cosmology: Principles and Applications of the General Theory of Relativity*. John Wiley & Sons, New York, 1972.

[20] D. Weiskopf and M. Ansorg. Visualization of the general relativistic rigidly rotating disk of dust. *Annalen der Physik*, 9:SI179–SI185, 2000.

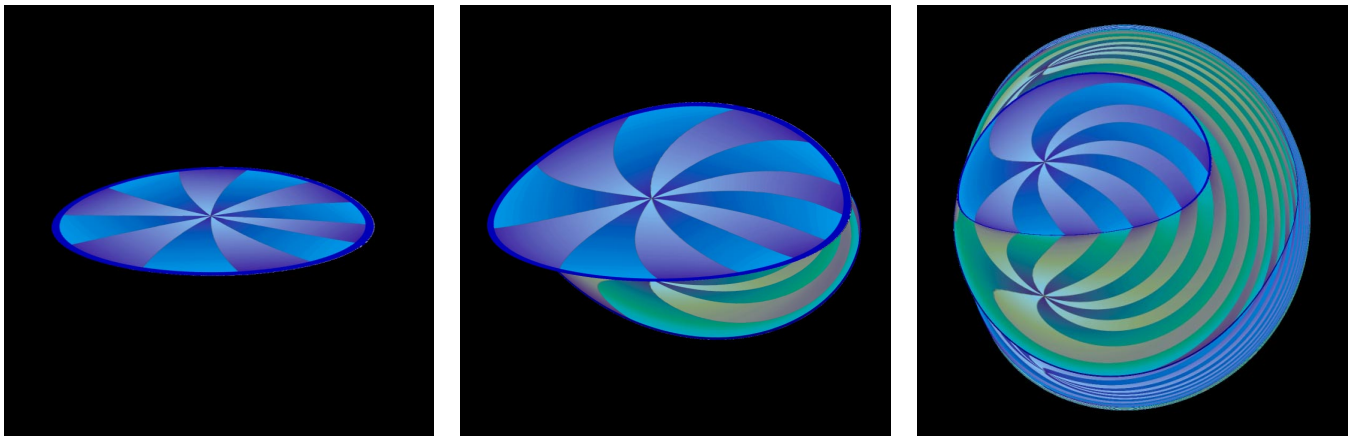

Figure 2: Visualization of the rigidly rotating disk of dust. The relativistic parameter μ is $0.1, 0.7, 3$, from left to right.

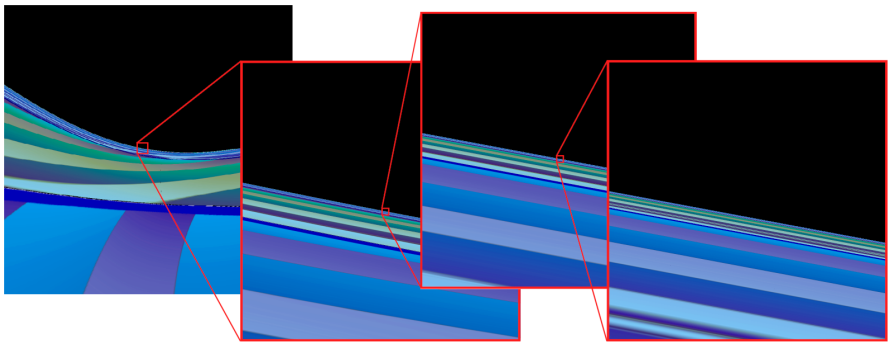

Figure 3: Fractal structures and self-similarity in the gravitational field of the rigidly rotating disk of dust with $\mu = 3$. The observer is located on the symmetry axis and is zooming in on the image.

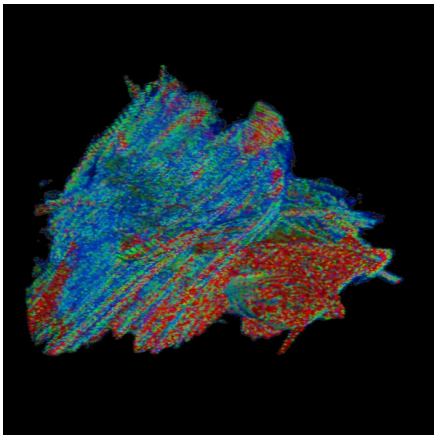

Figure 4: Caustic structure for $\mu = 0.3$.

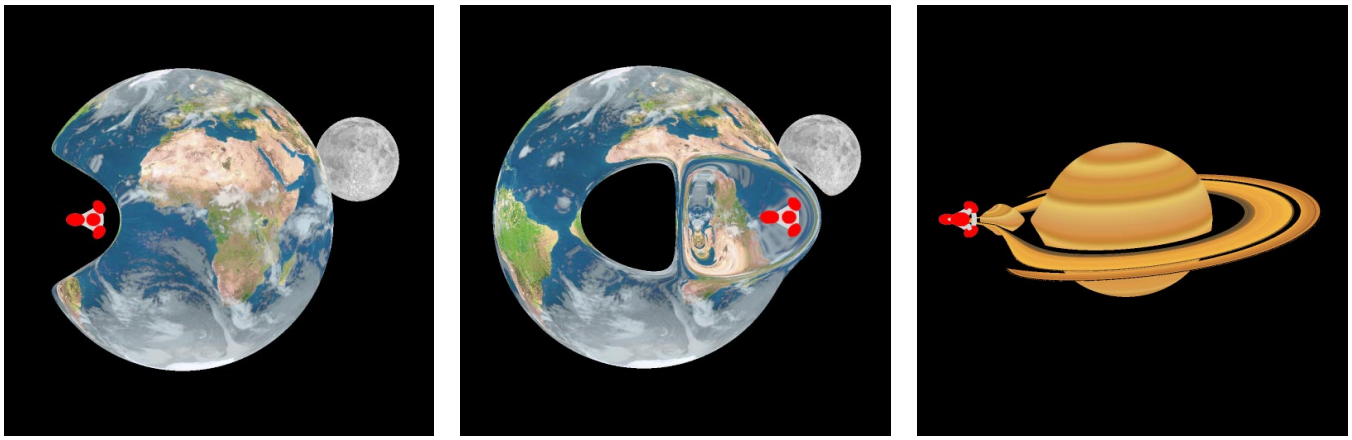

Figure 5: Visualization of the warp metric. The warp bubble and the spaceship are moving at a speed of $v = 1.5c$ in the left and middle image, and $v = 2.5c$ in the right image.